Published in final edited form as:
Nat Med. 2009 December ; 15(12): 1414–1420. doi:10.1038/nm.2050.

Synovial fibroblasts spread rheumatoid arthritis to unaffected joints

Stephanie Lefèvre[1], **Anette Knedla**[1], **Christoph Tennie**[1], **Andreas Kampmann**[1], **Christina Wunrau**[2], **Robert Dinser**[1], **Adelheid Korb**[3], **Eva-Maria Schnäker**[4], **Ingo H. Tarner**[1], **Paul D. Robbins**[5], **Christopher H. Evans**[6], **Henning Stürz**[7], **Jürgen Steinmeyer**[8], **Steffen Gay**[9], **Jürgen Schölmerich**[10], **Thomas Pap**[2], **Ulf Müller-Ladner**[1], and **Elena Neumann**[1]

[1]Department of Internal Medicine and Rheumatology, Justus-Liebig-University Giessen, Kerckhoff-Clinic, Bad Nauheim, Germany [2]Institute of Experimental Muskuloskeletal Medicine, University Hospital Muenster, Germany [3]Department of Internal Medicine D, Nephrology and Rheumatology, University Hospital Muenster, Germany [4]Department of Dermatology, University Hospital Muenster, Germany [5]Department of Microbiology and Molecular Genetics, University of Pittsburgh, School of Medicine, Pittsburgh, PA, USA [6]Center for Molecular Orthopedics, Harvard Medical School, Boston, MA, USA [7]Department of Orthopedics and Orthopedic Surgery, University Hospital Giessen and Marburg, Giessen, Germany [8]Deptment of Orthopedics and Experimental Orthopedics, University Hospital Giessen and Marburg Giessen, Germany [9]Center for Experimental Rheumatology, Zürich Center for Integrative Human Physiology, USZ, Zürich, Switzerland [10]Department of Internal Medicine I, University of Regensburg, Germany

Abstract

Active rheumatoid arthritis is characterized by originating from few but affecting subsequently the majority of joints. Thus far, the pathways of the progression of the disease are largely unknown. As rheumatoid arthritis synovial fibroblasts (RASFs) are key players in joint destruction and migrate *in vitro*, the current study evaluated the potential of RASFs to spread the disease *in vivo*. To simulate the primary joint of origin, healthy human cartilage was co-implanted subcutaneously into SCID mice together with RASFs. At the contralateral flank, healthy cartilage was implanted without cells. RASFs showed an active movement to the naïve cartilage *via* the vasculature independent of the site of application of RASFs into the SCID mouse, leading to a strong destruction of the target cartilage. These findings support the hypothesis that the characteristic clinical phenomenon of destructive arthritis spreading between joints is mediated, at least in part, by the transmigration of activated RASFs.

Corresponding author: Dr. Elena Neumann, Justus-Liebig-University Giessen, Dept Internal Medicine and Rheumatology, Kerckhoff-Klinik Bad Nauheim, Benekestr. 2-8, 61231 Bad Nauheim, Tel.: +49 6032 996 2801, Fax: +49 6032 996 2809, e.neumann@kerckhoff-klinik.de.

Author Contributions:
SL: Experiment selection, design and performance, manuscript preparation; AK: SCID-mouse surgery and evaluation; CT: Detection and evaluation of RASFs in mice; AK: LMM and evaluation of integrins; CW: TEER assay and evaluation; RD: Collagenase-injection and evaluation; AK: TEER, adhesion assay and evaluation; EMS: TEER assay and evaluation; IHT: SCID-mouse surgery; PDR and CHE: Preparation of adenoviral vectors; HS: Orthopedic surgery and collection for research; JSt: Tissue preparation for experiments; SG: Project design and experimental design; JSc; Project and experimental design; TP: Project and experimental design, TEER and adhesion assay; UML: Project development and design, experimental design, manuscript preparation; EN: Project development and coordination, study and experimental design and performance, manuscript preparation

Supplementary Information accompanies the paper on www.nature.com/nature.

Competing interests: The authors have no competing interests.

Introduction

Rheumatoid arthritis is a chronic inflammatory disease which leads to progressive joint destruction. It is characterized by synovial hyperplasia, cell activation, articular inflammation and invasion of the synovium into the adjacent bone and cartilage[1-3]. In most cases, the inflammatory process initially affects single joints, but the disease usually progresses to affect nearly all joints. The pathophysiology of rheumatoid arthritis involves numerous different cell-types, including macrophages, B-cells, T-cells, chondrocytes and osteoclasts, all of which contribute to the destructive process[4-8]. Research has accumulated a body of evidence that activated synovial fibroblasts (SFs), which are present in large numbers in rheumatoid synovium, are one of the key players in the destructive process of rheumatoid arthritis[9]. Of the various pathogenic pathways mediated by this cell-type, RASFs contribute primarily to the progression of the disease by attaching to, invading into and degrading cartilage and bone[2,3,10-12].

RASFs drive the destruction of articular cartilage by the production of matrix degrading enzymes through upregulation of adhesion molecules and subsequent attachment to cartilage. To simulate and analyze these properties, the severe combined immunodeficiency (SCID) mouse model of rheumatoid arthritis has been developed[9,13]. Although it does not reflect the complete process of the development of rheumatoid arthritis, the SCID mouse model facilitates the study of distinct pathophysiologic mechanisms including interactions of isolated human RASFs or whole synovial tissue with healthy human cartilage *in vivo*.

Lacking cellular and humoral immune responses, SCID mice are not able to reject xenograft implants. When normal human cartilage and human RASFs[13] or rheumatoid arthritis synovium are co-implanted subcutaneously, the progression of the cartilage invasion of RASFs and perichondrocytic degradation can be observed in the absence of a murine adaptive immune system and human immune cells and mediators over an extended period of time[9,12-14].

One of the unique clinical characteristics of rheumatoid arthritis is the continuous spreading of disease, which usually starts in single joints and eventually progresses to involve the majority of joints. It has long been speculated that this phenomenon is due to a circulation of humoral or cellular factors, although no conclusive data have been obtained from serum or immune cell transfer models.

This study shows that one of the key players in matrix degradation, the mesenchymal RASF, is not only able to invade and degrade cartilage without additional stimuli from a murine adaptive and the human immune system but also to maintain and transfer its properties to a distant and hitherto unaffected joint. This migratory potential has been known from short-range situations such as wound healing[15-19], but long-distance migration has not been demonstrated in a human-like experimental setting.

Results

Migration of RASFs *in vivo*

RASFs attached to, invaded into and degraded cartilage which was co-implanted simultaneously with RASFs in the SCID mouse model of rheumatoid arthritis [Fig. 1a][12-14]. Multiple areas of directed, invasive growth of RASFs into the implanted cartilage and perichondrocytic cartilage degradation were observed [Fig. 1b, c]. Scores are summarized in Table 1.

RASFs were not only able to invade and degrade coimplanted cartilage (primary implant); they also migrate to the contralaterally implanted human cartilage that had been inserted without RASFs and maintained their ability to invade and degrade the cartilage [Fig. 1d]. Invasion and degradation scores at the contralateral side were slightly lower than those of the primary implant [Fig. 1b].

As a control, osteoarthritis (OA) SFs were implanted instead of RASFs together with human cartilage [Supplementary Figure 1]. In a second approach, cartilage was inserted without adding RASFs or OASFs. In both cases, no invasion could be observed [Fig. 1b]. Invasion score of RASFs compared to OASFs: $p= 3.67*10^{-7}$ ($p < 0.001$).

To confirm that invading cells were of human origin and migrated through the murine body, species-specific immunohistochemistries were performed. Alternatively, fluorescence of EGFP-transduced RASFs was detected.

The invading cells at the contralateral implant were positive for human vimentin, follistatin and proMMP-13 [Fig. 1e, f]. Murine IL-1 receptor and $H\text{-}2D^d$ were not detectable at the invasion zone [Fig. 1g, Supplementary Figure 1] confirming that all invading cells were of human origin.

To evaluate potential influences of the surgical procedure and wound healing on the migratory capability, RASF-containing (primary) and RASF-free (contralateral) cartilage-sponge complexes were implanted at different timepoints.

1. Implantation of the primary implant followed by implantation of the contralateral cartilage after 14 days. Scores of the primary implant: 2.7±0.4 (inv) and 2.5±0.7 (deg); contralateral implant: 1.5±0.6 (inv) and 1.7±0.8 (deg) [Table 1]. Invasion score of the primary RASF-containing implant was significantly higher in comparison to the contralateral RASF-free implant $p = 4.16*10^{-10}$ ($p < 0.001$).
2. Implantation of the contralateral RASF-free implant followed by implantation of the primary complex after 14 days. Scores of the contralateral implant: 2.8±0.5 (inv) and 2.5±0.7 (deg); primary implant: 1.8±0.7 (inv) and 2.3±0.7 (deg) [Table 1]. Invasion score of the contralateral RASF-free implant was significantly higher in comparison to the primary RASF-containing implant: $p = 1.3*10^{-8}$ ($p < 0.001$).

Invasion and degradation scores of the RASF-free contralateral implants were significantly higher when implanted first in comparison to the contralateral implant that was implanted after 14 days (invasion: $p = 2.0*10^{-12}$; degradation: $p = 3{,}5*10^{-4}$).

No significant difference was observed between the RASF-containing implants of both experimental settings.

Injection of RASFs

To analyze the route of migration of RASFs to the implanted cartilage and influences of wound healing, RASFs were injected subcutaneously (s.c.), intraperitoneally (i.p.) and intravenously (i.v.) 14 days after cartilage implantation. RASF injection led to the destruction of the implanted cartilage, particularly after subcutaneous and intravenous application [Supplementary Figure 1] corresponding to the scores of simultaneous cartilage-RASF implantation [Fig. 2a]. Destruction of the implanted cartilage was slightly lower after intraperitoneal injection [Fig. 2a]. Scores are summarized in Table 1.

In addition, RASFs were injected 14 days prior to the implantation of cartilage. The cells still invaded and degraded the cartilage. Scores were lower when cartilage was implanted

first followed by RASF injection. To confirm early neovascularization, vessel formation was analyzed and detectable at day 14 and even at day 7 *post* implantation [Fig. 2b].

Role of synovium, chondrocytes and ECM

To determine whether other human synovial cells and extracellular matrix (ECM) influence the migratory potential of RASFs, complete synovial tissue was implanted as a natural source of RASFs. The implantation of whole synovium resulted in the migration of RASFs out of the synovium towards the contralateral cartilage implant in 9 out of 15 animals [Figs. 2a, c]. There was an extensive invasion of RASFs into the cartilage and strong perichondrocytic degradation [Table 1].

To investigate whether viable chondrocytes are necessary for RASF migration towards human cartilage, chondrocytes were devitalized prior to implantation [Supplementary Figure 1]. Strong invasion and perichondrocytic degradation of RASFs into the chondrocyte-depleted cartilage were observed [Table 1; Fig. 2a].

Bovine or murine cartilage, respectively, was co-implanted with RASFs to analyze the role of the ECM [Fig. 2d; Supplementary Figure 1]. A strong destruction of the cartilage was seen in bovine [Table 1; Fig. 2a] and in matrix exposed murine cartilage. Interestingly, RASF invasion was mainly visible at the cartilage bone junction [Fig. 2d].

Route of migration and role of cartilage

In order to further elucidate the route of migration, internal organs were analyzed [Table 2]. Single fibroblasts were detectable in the skin at the site of implantation in one animal [Fig. 3a]. The majority of RASFs was found in the spleen [Fig. 3b]. Single cells were found in the kidney and a lymph node in one animal. RASFs were not detectable in the intestine [Fig. 3c], lung, heart, liver or skin distant from the implant [Fig. 3a].

To evaluate whether RASFs are also able to migrate to murine cartilage, murine auricular cartilage and joints were examined by immunohistochemistry [Table 2].

In 2 out of 18 animals (11%), human cells were detected in healthy, untreated murine joints [Fig. 3a].

RASFs were found in the auricular cartilage in 8 of 20 mice (40%) [Fig. 3a]. 6 of these 8 RASF-positive cartilage specimens showed single, the two remaining specimens 10 - 50 human cells.

A collagenase-induced OA mouse model was used[20] to analyze whether local cartilage damage leads to attachment and invasion of RASFs compared to healthy murine joints,. Histological and immunohistological analyses showed untypical invasive erosions into cartilage and bone in animals with injected RASFs in contrast to animals without RASFs at all time points [Fig. 3d, Supplementary Figure 2].

To confirm the ability of RASFs to adhere to damaged cartilage matrix *in vitro*, OASFs and RASFs were seeded on collagenase-treated and non-treated murine cartilage explants. OASFs did not attach to untreated cartilage whereas RASFs showed a slight attachment to freshly isolated but untreated murine cartilage [Fig. 3e]. Collagenase-treatment of the cartilage significantly increased the attachment of SFs with RASFs showing a markedly higher adhesion towards the murine cartilage [Fig. 3e].

To analyze whether RASFs are able to access the bloodstream and use this pathway for migration, blood was collected on the day of sacrifice and examined *via*

immunocytochemistry for the presence of human cells. RASFs were detected in the isolated blood in 43% of the animals [Fig. 3f, Supplementary Figure 3]. Cells were applied intravenously in 25% of the RASF-positive animals, subcutaneously in 10% and intraperitoneally in 8%.

Additional PCR-analysis of the y-chromosome gene *sry* from RASFs from male patients implanted together with healthy cartilage from female patients into female SCID mice showed the human origin of circulating cells in the isolated murine blood [Fig. 3g].

Adhesion molecules at the invasion zone

As RASFs have an increased potential to adhere to damaged cartilage matrix, the expression of adhesion molecules was analyzed by real time PCR after laser-mediated microdissection (LMM) of the invasion zone. Integrin subunits α2, α4, αν, β1 and β5 were expressed at the sites of invasion [Fig. 3h]. No difference was seen between primary and contralateral implants. Non-invading cells in the surrounding sponge showed identical expression patterns. The integrin subunits β1 and β5 were also strongly expressed in cultivated RASFs at RNA- and protein level (data not shown). The expression of the integrin subunit αν was confirmed by immunohistochemistry [Supplementary Figure 4].

Migration and adhesion of RASFs *in vitro*

Transmigration through confluent cell layers is an important prerequisite for entering and leaving the bloodstream at sites of the disease or distant locations. To investigate whether RASFs, similarly to tumor cells, are able to transmigrate, the transepithelial electrical resistance (TEER) assay was used. The breakdown of the electrical resistance generated by a MDCK-C7 cell monolayer as invasive cells transmigrate was measured[21].

RASFs exhibited a strong transmigration through the monolayer comparable to Cal78 chondrosarcoma cells. Two days after adding RASFs onto MDCK-C7 cells, the resistance decreased to more than 60% of the baseline value. Total breakdown was achieved after 3-4 days [Fig. 4a]. Human skin fibroblasts (HSFs) and OASFs did not show this invasive behavior [Fig. 4a].

Cellular adhesion of RASFs was blocked using anti-VCAM-1 antibodies. After an adhesion time of 4 min, a decreased number of adhered RASFs was observed compared to untreated RASFs [Fig. 4b].

Using the TEER assay, the influence of BB-94 and TIMP-3 on the transmigration of RASFs was analyzed. BB-94 treated or TIMP-3 transduced RASFs showed a reduced transmigratory potential compared to the controls [Figs. 4c, d].

In vivo, application of TNFα-inhibitors (40 mg/kg body weight, every 10 or 14 days, i.p. or s.c.) did not result in protective effect towards RASF migration and subsequent cartilage invasion in this migration model [Table 1].

Discussion

Rheumatoid arthritis starts in a few joints but can involve all joints during the course of the disease. This study addressed one of the remaining questions of rheumatoid arthritis, the mechanisms and effector cells that lead to this characteristic clinical feature of progressive joint affection. We could show that RASFs are able to migrate long distances through the blood stream in the SCID mouse model for rheumatoid arthritis and specifically migrate towards, attach to, and invade into distant exposed cartilage matrix.

RASFs have the ability to remodel mesenchymal structures, mediated by the production of cytokines, chemokines, matrix components and MMPs[2,3,13,15]. This ability has also been demonstrated in wound healing[15-19], which induces a change from the "resting" to the "activated" phenotype of the fibroblast[18]. This activation includes the limited ability to migrate short distances since fibroblasts are regarded as resident cells[15,16,21]. In our SCID-mouse model, RASFs undergo the complex process of emigration from an affected joint (simulated by an RASF-containing cartilage complex), migration into a healthy joint (simulated by a RASF-free cartilage implant), and subsequent invasion of articular cartilage [Fig. 1]. This ability to migrate clearly exceeds a short-ranged intra-organ movement. These properties appear to be unique to RASFs, as OASFs and HSFs neither invaded or degraded human cartilage [Fig. 1, Supplementary Figure 1, Table 1]; they also lacked the transmigratory capacity [Fig. 4].

Migration of RASFs is not dependent on active tissue damage and beginning wound healing as application of RASFs 14 days after implantation also resulted in strong cartilage destruction [Table 1]. Progressed or completed wound healing and established vascularization appear to promote RASF migration and adhesion to the implanted cartilage independent of the way of application [Fig. 2a, Supplementary Figure 1, Table 1].

RASF migration towards the cartilage takes place through the blood stream [Figs. 3f, g, Supplementary Figure 3]. Cells migrating through the blood pass the spleen, which is an important filter system of the circulation and is the only internal organ, where RASFs were detected in all animals [Fig. 3b, Table 2]. High numbers of RASFs accumulated in the RASF-free human cartilage implants independent of the way of application [Table 1]. The transmigratory capacity of RASFs was also illustrated by their transmigration into the implants after i.p. injection [Table 1]. In addition, RASFs may not be able to survive over long periods of time in other tissues when they can not attach to cartilage matrix. Therefore, RASFs were detectable at sites of invasion and in the blood but not in organs except the spleen [Figs. 1, 3a-c, f, g, Table 2].

The transmigratory potential of RASFs through endothelial and epithelial cell layers was confirmed *in vitro* [Fig. 4]. Angiogenesis seems to be an important feature for the migration of RASFs to a distant part of the body. In our model, neovascularization into the implants was detected already seven days after implantation [Fig. 2b] facilitating the early transmigration of RASFs into the vascular system. In addition, murine vascular activation may render the implanted cartilage more vulnerable as RASF migration takes place through the blood stream [Supplementary Figure 4].

To evaluate whether the migratory capacity could be an acquired feature of isolated RASFs after *in vitro* culture, complete rheumatoid synovium was implanted instead of isolated RASFs. Similar to the RASF implantation, an impressive invasion of the healthy cartilage was observed, even though the number of RASFs in the synovial tissue samples was much lower than those in the sponge implants [Fig. 2c, Table 1]. Thus, RASFs are able to actively leave their "normal" synovial environment and subsequently exert their migratory and destructive capacity.

The factors leading to the specific migration and attachment of RASFs to cartilage are important features of RASF spreading. Obviously, vital chondrocytes and chondrocyte derived chemokines and other factors are not necessary for RASF migration [Fig. 2a, Supplementary Figure 1]. However, matrix components, small matrix fragments as well as other matrix-associated proteins in the ECM such as chemokines and growth factors may drive the migration of RASFs towards the "accessible" implanted cartilage, even in the absence of factors actively produced by chondrocytes [Supplementary Figure 1][22-28].

Adhesion molecules such as VCAM-1 and integrins are increased in rheumatoid arthritis tissue[29-33] and may be important mediators of RASF transmigration into the vascular system and invasion into the cartilage. In our model, RASFs express integrins at sites of invasion [Fig. 3h, Supplementary Figure 4]. The inhibition of VCAM-1 reduced the migration of RASFs through confluent cell layers [Fig. 4]. In contrast, the inhibition of key inflammatory factors known to be involved in rheumatoid arthritis pathophysiology such as TNFα was not able to reduce RASF migration [Table 2].

Although we could show that RASFs are able to invade cartilage of other species [Fig. 2d, Supplementary Figure 1], only a limited number of RASFs was detected in healthy murine joints or articular cartilage of the SCID mice [Table 2]. A reason for the limited invasion into healthy joints may be the intact tissue structure. The capsule, the separation of the different tissue compartments and the limited contact of the synovial tissue to cartilage and bone separated by the synovial space appears to be the natural protection barrier for an invasion of RASFs[1,11,13]. Therefore, invasion of RASFs into non-affected joints most likely requires microlesions to initiate the attachment of RASF to the matrix. This theory is in accordance with the observation of early erosions at the cartilage-bone-junction in diseased individuals and the preference for disease manifestations in the dominant hand. Here, the synovial lining layer is in close proximity and - in part - in direct contact with cartilage and bone[34-36], similar to the situation in our experimental model, in which invasion of RASFs was prominent at cartilage-bone-junctions [Fig. 2d]. To further clarify this issue, cartilage damage was induced *in vivo* by collagenase and RASF application. Interestingly, untypical erosions for the OA model used were observed, similar to erosions in human rheumatoid arthritis [Fig. 3d, Supplementary Figure 2]. Additionally, the increased attachment of RASFs to collagenase-treated cartilage was confirmed *in vitro* [Fig. 3e].

Taken together, the results support the idea that RASFs are one of the key pathophysiologic factors that facilitate and drive the progression from oligo- to polyarticular disease in rheumatoid arthritis, which is based on the unique potential of the RASFs to migrate *via* the vasculature towards hitherto unaffected cartilage.

Methods

Tissues and cells

Rheumatoid arthritis ($n = 17$) and OA ($n = 6$) synovial tissues were obtained during arthroplastic surgery (approved by: Ethics Committee Universities of Giessen and Muenster). Patients gave informed consent and fulfilled the criteria of the American College of Rheumatology[37]. RASF ($n = 14$), OASF ($n = 6$) were isolated and cultured (max. 5 passages)[12,38-39].

Healthy human cartilage ($n = 38$) from non-arthritic knee joints and complete arthritic synovial tissue ($n = 3$) was obtained on the day of implantation. Healthy bovine joints were received from a butchery and the Cal78 chondrosarcoma cell line from DMSZ (Braunschweig, Germany).

Mice

Female 5-wks-old Crl-scidBR and wild-type mice (Charles River) were housed under germ-free conditions. Experiments were approved by the Animal Care and Use Committee of Hesse.

Adenoviral transduction

cDNA of enhanced green fluorescent protein (EGFP) was inserted into replication-deficient type5 adenoviruses (ΔE1/E3)[40] under control of a cytomegalovirus (CMV) promotor. 30 multiplicity of infection were added to 5×10^5 RASF, incubated (37°C, 2 h), washed, and cultured until implantation[12]. Infection rate: 95% with decreasing EGFP expression (day 60: 10-25%).

SCID-mouse model

RASFs were co-implanted with cartilage[41]. Alternatively, bovine cartilage or healthy articular heads with scraped surface of shoulders/hips from donor mice, or devitalized cartilage[42] was implanted. One sponge including cartilage and fibroblasts was inserted subcutaneously into a SCID-mouse (primary), another cell-free cartilage-sponge complex contralaterally [Fig. 1a]. No difference in invasion between gelatine-sponges and plasticpolymer-sponges was observed (not shown). Controls: Implantation of synovial tissue (primary) and human cartilage (contralateral); time-displaced implantation of primary and contralateral implants (14 days); injection of fibroblasts i.v., s.c. or i.p 14 days *after/prior* to RASF-free implantation. Adalimumab (40 mg/kg body weight, Abbott Laboratories, Wiesbaden, Germany) was injected s.c. or i.p. every 14 or 10 days, respectively.

After 60 days, blood was collected, implants and organs were snap-frozen, implanted articular heads were decalcified and embedded in paraffin. Early neovascularization was analyzed at day 7 and 14.

Collagenase (5 U; Sigma, Deisenhofen, Germany) was injected intraarticularily [20] and RASFs applied s.c. After 28, 39, 67 days, joints were removed and embedded in paraffin.

Implant evaluation was performed using stained sections to determine fibroblast invasion/ perichondrocytic cartilage degradation[11,14, 38,43].

Immunohistochemistry of organs: RASFs directly coimplanted ($n = 5$), implanted time-displaced ($n = 2$), injected ($n = 4$ subcutaneous, intraperitoneal, intravenous each) or using bovine cartilage ($n = 1$).

Immunohistochemistry

Antibodies for frozen sections: mouse-anti-human vimentin (1:100; Dako, Hamburg, Germany); mouse-anti-human follistatin, goat-anti-human proMMP-13 (1:100; R&Dsystems); mouse-anti-human integrin αν (1:100; Chemicon, Hofheim, Germany); mouse-anti-mouse H-2D^d (1:50; BD-Biosciences, Heidelberg, Germany), goat-anti-mouse IL-1 receptor (1:25; R&Dsystems). Detection was performed with Histofine Simple-Stain MAX/PO anti-mouse/rabbit/goat (Medac, Wedel, Germany) or secondary antibodies (BD-Biosciences) and AEC-substrate (VectorLaboratories, Burlingame, CA, USA).

Paraffin sections were incubated with anti-human vimentin and -mouse H-2D^d antibodies after proteinase K damasking. Positive control: Rheumatoid arthritis synovium. After erythrocyte lysis (QIAGEN, Hilden, Germany), blood cells were harvested onto slides using a cytospin centrifuge, fixed and analyzed immunocytochemically.

Laser-mediated microdissection (LMM)

LMM was performed using a Robot-MicroBeam laser microscope (P.A.L.M. Microlaser Technologies)[44-46]. RNA was extracted from 10,000 cartilage invading cells (PicoPure RNA Isolation-Kit, Arcturus, Sunnyvale, CA, USA).

PCR

RASFs from male patients were co-implanted with female human cartilage. DNA of murine blood was isolated (QIAamp DNA Blood-Kit, QIAGEN) and concentrated (Microcon, Millipore, Bedford, MA, USA). Standard-amplification was performed (50°C annealing temperature, T_a), purified and reamplified. Controls: human male, female DNA, distilled water. Primers: Human *sry* 5'-GCGTATTCAACAGCGATGATTACAG-3', 5'-GTTACCCGATTGTCCTACAGCTTTG-3'. For Real time PCR, cDNA was synthesized and integrin-expression after LMM analyzed (LightCycler, Roche)[44]. Endogenous control: porphobilinogen deaminase. Primers: Integrin-α2: 5'-AGAAGTCTGTTGCCTGCGAT-3', 5'-CTTGGAAACTGAGAGACGCC-3', T_a: 50°C; integrin-α4: 5'-AAATGGATGGCCTTCTGTG-3', 5'-TCTTGGTGGAGACTCTGCCT-3', T_a: 48°C; integrin-β1: 5'-ATCCCAGAGGCTCCAAAGAT-3', 5'-CCCCTGATCTTAATCGCAAA-3', T_a: 50°C; integrin-β5: 5'-TGCCTTGCTTGGAGAGAAAT-3', 5'-AATCTCCACCGTTGTTCCAG-3', T_a: 50°C.

Transepithelial electrical resistance (TEER) assay

800,000 cells were added onto a MDCK-C7 monolayer[21]. Cellular invasion was determined in quadruplicate through TEER until total breakdown.

Human umbilical vein endothelial cells (HUVEC) on gelatine-coated glass coverslips were placed upon a microchip (microfluidic device, 146 MHz, 1 dBm) to generate a laminar flow. 3,000 stained RASFs were added and attached RASFs quantified after 4 min. Treatments: anti-VCAM-1 antibodies (50 ng/ml, 2h; abcam; $n = 3$, control $n = 4$; primary culture of one patient); 100 ng/ml BB94 (untreated RASFs: $n = 2$; RASFs/BB94: $n = 2$; primary culture of one patient); nonviral expression construct (pFlagCMV-2) encoding TIMP-3, 10 h after lipofection (Lipofectamine2000; Invitrogen; untreated RASFs: $n = 2$; MOCK: $n = 4$; TIMP3: $n = 4$; primary culture of two patients).

Attachment assay

Murine femoral head cartilage was isolated[47] and cultured (DMEM, 37°C, 5 % CO_2; 24h). RASFs and OASFs[48] were placed on proteoglycan-reduced cartilage (0.25 mg/ml collagenase, 4 h)[49] for 2 h under rotation, cultured for 12h, fixed, and attached cells quantified.

Statistics

Parametric data: *t* test. Non-parametric data: Mann-Whitney test. Significance: *P*-values <0.05.

Acknowledgments

This study was funded by a start-up grant of the German Society of Rheumatology (DGRh) and by a research grant of the German Research Foundation (DFG: NE1174/3-1, MU1383/14-1, FOR 696). We wish to thank Simone Benninghoff, Birgit Riepl, Sabrina Brückmann, and Carina Schreiyäck for technical assistance.

References

1. Karouzakis E, Neidhart M, Gay RE, Gay S. Molecular and cellular basis of rheumatoid joint destruction. Immunol Lett. 2006; 106:8–13. [PubMed: 16824621]
2. Muller-Ladner U, Pap T, Gay RE, Neidhart M, Gay S. Mechanisms of disease: the molecular and cellular basis of joint destruction in rheumatoid arthritis. Nat Clin Pract Rheumatol. 2005; 1:102–10. [PubMed: 16932639]

3. Pap T, Muller-Ladner U, Gay RE, Gay S. Fibroblast biology. Role of synovial fibroblasts in the pathogenesis of rheumatoid arthritis. Arthritis Res. 2000; 2:361–7. [PubMed: 11094449]
4. Gravallese EM. Bone destruction in arthritis. Ann Rheum Dis. 2002; 61(Suppl 2):ii84–6. [PubMed: 12379632]
5. Looney RJ. B cell-targeted therapy for rheumatoid arthritis: an update on the evidence. Drugs. 2006; 66:625–39. [PubMed: 16620141]
6. Ma Y, Pope RM. The role of macrophages in rheumatoid arthritis. Curr Pharm Des. 2005; 11:569–80. [PubMed: 15720276]
7. Skapenko A, Leipe J, Lipsky PE, Schulze-Koops H. The role of the T cell in autoimmune inflammation. Arthritis Res Ther. 2005; 7(Suppl 2):S4–14. [PubMed: 15833146]
8. Yasuda T. Cartilage destruction by matrix degradation products. Mod Rheumatol. 2006; 16:197–205. [PubMed: 16906368]
9. Pap T, Meinecke I, Muller-Ladner U, Gay S. Are fibroblasts involved in joint destruction? Ann Rheum Dis. 2005; 64(Suppl 4):iv52–4. [PubMed: 16239388]
10. Buckley CD, et al. Fibroblasts regulate the switch from acute resolving to chronic persistent inflammation. Trends Immunol. 2001; 22:199–204. [PubMed: 11274925]
11. Huber LC, et al. Synovial fibroblasts: key players in rheumatoid arthritis. Rheumatology (Oxford). 2006; 45:669–75. [PubMed: 16567358]
12. Neumann E, et al. Inhibition of cartilage destruction by double gene transfer of IL-1Ra and IL-10 involves the activin pathway. Gene Ther. 2002; 9:1508–19. [PubMed: 12407423]
13. Muller-Ladner U, et al. Synovial fibroblasts of patients with rheumatoid arthritis attach to and invade normal human cartilage when engrafted into SCID mice. Am J Pathol. 1996; 149:1607–15. [PubMed: 8909250]
14. Muller-Ladner U, et al. Human IL-1Ra gene transfer into human synovial fibroblasts is chondroprotective. J Immunol. 1997; 158:3492–8. [PubMed: 9120311]
15. Garcia-Vicuna R, et al. CC and CXC chemokine receptors mediate migration, proliferation, and matrix metalloproteinase production by fibroblast-like synoviocytes from rheumatoid arthritis patients. Arthritis Rheum. 2004; 50:3866–77. [PubMed: 15593223]
16. Takahara K, et al. Autocrine/paracrine role of the angiopoietin-1 and -2/Tie2 system in cell proliferation and chemotaxis of cultured fibroblastic synoviocytes in rheumatoid arthritis. Hum Pathol. 2004; 35:150–8. [PubMed: 14991531]
17. Woods JM, et al. A cell-cycle independent role for p21 in regulating synovial fibroblast migration in rheumatoid arthritis. Arthritis Res Ther. 2006; 8:R113. [PubMed: 16846525]
18. van Beurden HE, Snoek PA, Von den Hoff JW, Torensma R, Kuijpers-Jagtman AM. Fibroblast subpopulations in intra-oral wound healing. Wound Repair Regen. 2003; 11:55–63. [PubMed: 12581427]
19. Clark RAF, An JC, Greiling D, Khan A, Schwarzbauer JE. Fibroblast migration on fibronectin requires three distinct functional domains. J Invest Dermatol. 2003; 121:695–705. [PubMed: 14632184]
20. Blaney Davidson EN, et al. Resemblance of osteophytes in experimental osteoarthritis to transforming growth factor β-induced osteophytes. Arthritis Rheum. 2007; 56:4065–73. [PubMed: 18050218]
21. Zak J, Schneider SW, Eue I, Ludwig T, Oberleithner H. High-resistance MDCK-C7 monolayers used for measuring invasive potency of tumour cells. Pflugers Arch. 2000; 440:179–83. [PubMed: 10864013]
22. Hutchings H, Ortega N, Plouet J. Extracellular matrix-bound vascular endothelial growth factor promotes endothelial cell adhesion, migration, and survival through integrin ligation. Faseb J. 2003; 17:1520–2. [PubMed: 12709411]
23. Hubbell JA. Matrix-bound growth factors in tissue repair. Swiss Med Wkly. 2007; 137(Suppl 155): 72S–76S. [PubMed: 17874506]
24. Hall H, Hubbell JA. Matrix-bound siwth Ig-like domain of cell adhesion molecule L1 acts as an angiogenic factor by ligating alphavbeta3-integrin and activating VEGF-R2. Microvasc Res. 2004; 68:169–78. [PubMed: 15501236]

25. Cazes A, et al. Extracellular matrix-bound angiopoietin-like 4 inhibits endothelial cell adhesion, migration, and sprouting and alters actin cytoskeleton. Circ Res. 2006; 99:1207–15. [PubMed: 17068295]
26. Felix R, et al. Synthesis of membrane- and matrix-bound colony-stimulating factor-1 by cultured osteoblasts. J Cell Physiol. 1996; 166:311–22. [PubMed: 8591991]
27. Nicosia RF, Tuszynski GP. Matrix-bound thrombospondin promotes angiogenesis in vitro. J Cell Biol. 1994; 124:183–93. [PubMed: 7507491]
28. Saint-Geniez M, Kurihara T, D'Amore PA. Absence off cell and matrix-bound VEGF isoforms is associated with abnormal lens development. Invest Ophthalmol Vis Sci. 2008
29. el-Gabalawy H, et al. Synovial distribution of alpha d/CD18, a novel leukointegrin. Comparison with other integrins and their ligands. Arthritis Rheum. 1996; 39:1913–21. [PubMed: 8912515]
30. Morales-Ducret J, et al. Alpha 4/beta 1 integrin (VLA-4) ligands in arthritis. Vascular cell adhesion molecule-1 expression in synovium and on fibroblast-like synoviocytes. J Immunol. 1992; 149:1424–31. [PubMed: 1380043]
31. Muller-Ladner U, et al. Alternatively spliced CS-1 fibronectin isoform and its receptor VLA-4 in rheumatoid arthritis synovium. J Rheumatol. 1997; 24:1873–80. [PubMed: 9330926]
32. Schedel J, et al. Differential adherence of osteoarthritis and rheumatoid arthritis synovial fibroblasts to cartilage and bone matrix proteins and its implication for osteoarthritis pathogenesis. Scand J Immunol. 2004; 60:514–23. [PubMed: 15541045]
33. Giancotti FG, Ruoslahti E. Integrin signaling. Science. 1999; 285:1028–32. [PubMed: 10446041]
34. Ishikawa H, Ohno O, Hirohata K. An electron microscopic study of the synovial-bone junction in rheumatoid arthritis. Rheumatol Int. 1984; 4:1–8. [PubMed: 6718949]
35. Bromley M, Bertfield H, Evanson JM, Woolley DE. Bidirectional erosion of cartilage in the rheumatoid knee joint. Ann Rheum Dis. 1985; 44:676–81. [PubMed: 4051589]
36. Bresnihan B. Pathogenesis of joint damage in rheumatoid arthritis. J Rheumatol. 1999; 26:717–9. [PubMed: 10090189]
37. Arnett FC, et al. The American Rheumatism Association 1987 revised criteria for the classification of rheumatoid arthritis. Arthritis Rheum. 1988; 31:315–24. [PubMed: 3358796]
38. Muller-Ladner U, et al. Gene transfer of cytokine inhibitors into human synovial fibroblasts in the SCID mouse model. Arthritis Rheum. 1999; 42:490–7. [PubMed: 10088772]
39. Neumann E, et al. Identification of differentially expressed genes in rheumatoid arthritis by a combination of complementary DNA array and RNA arbitrarily primed-polymerase chain reaction. Arthritis Rheum. 2002; 46:52–63. [PubMed: 11817609]
40. Lechman ER, et al. Direct adenoviral gene transfer of viral IL-10 to rabbit knees with experimental arthritis ameliorates disease in both injected and contralateral control knees. J Immunol. 1999; 163:2202–8. [PubMed: 10438962]
41. Judex M, et al. "Inverse wrap" - an improved implantation technique for virus-transduced synovial fibroblasts in the SCID-mouse model for RA. Mod Rheumatol. 2001; 11:145–150.
42. Clements KM, Bee ZC, Crossingham GV, Adams MA, Sharif M. How severe must repetitive loading be to kill chondrocytes in articular cartilage? Osteoarthritis Cartilage. 2001; 9:499–507. [PubMed: 11467899]
43. Knedla A, et al. The therapeutic use of osmotic minipumps in the SCID mouse model for rheumatoid arthritis. Ann Rheum Dis. 2008 Epub ahead of print.
44. Hashimoto A, et al. Laser-mediated microdissection for analysis of gene expression in synovial tissue. Mod Rheumatol. 2007; 17:185–90. [PubMed: 17564772]
45. Judex M, Neumann E, Gay S, Muller-Ladner U. Laser-mediated microdissection as a tool for molecular analysis in arthritis. Methods Mol Med. 2004; 101:93–105. [PubMed: 15299212]
46. Lechner S, et al. Gene expression pattern of laser microdissected colonic crypts of adenomas with low grade dysplasia. Gut. 2003; 52:1148–53. [PubMed: 12865273]
47. Little CB, et al. ADAMTS-1-knockout mice do not exhibit abnormalities in aggrecan turnover in vitro or in vivo. Arthritis Rheum. 2005; 52:1461–72. [PubMed: 15880348]

48. Van der Laan WH, et al. Cartilage degradation and invasion by rheumatoid synovial fibroblasts is inhibited by gene transfer of a cell surface-targeted plasmin inhibitor. Arthritis Rheum. 2000; 43:1710–18. [PubMed: 10943860]

49. Hajiioannou J, et al. In vitro enzymatic treatment and carbon dioxide laser beam irradiation of morphologic cartilage specimens. Arch Otolaryngol Head Neck Surg. 2006; 132:1363–70. [PubMed: 17178949]

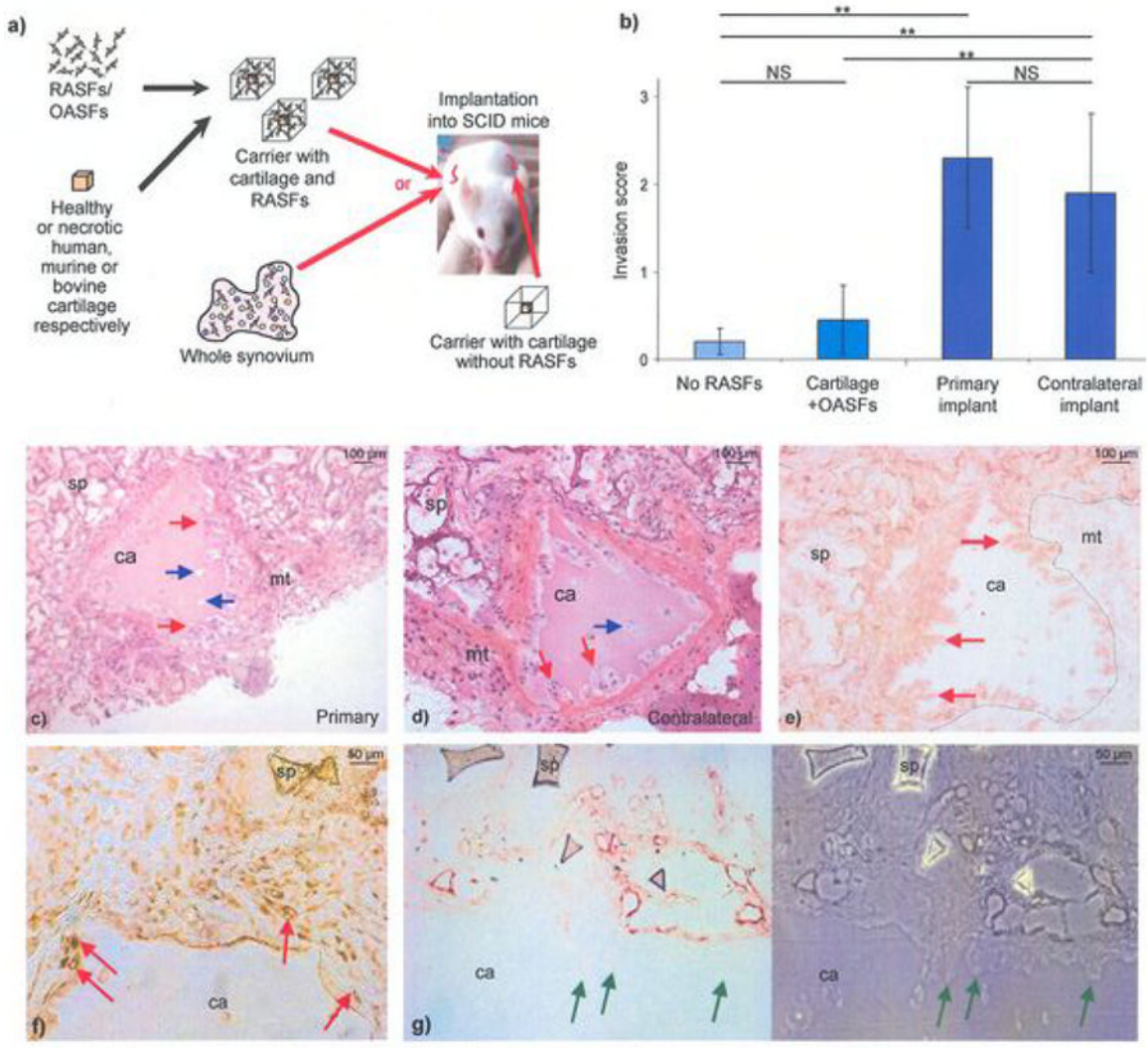

Figure 1. Migration of RASFs

(a) Cartilage-sponge complexes with or without RASFs were implanted into SCID mice at opposite sites. OASFs, human synovium, necrotic human, bovine or murine cartilage served as controls. (b) Invasion scores show a deep invasion of RASFs in the primary and contralateral implant. Limited cartilage invasion by OASFs or into RASF-free cartilage was observed. *p<0.05; **p<0.001; NS: not significant. (c, d) Histology shows RASF invasion and pc degradation at the primary and contralaterally implanted cartilage (red arrows: invasion; blue arrows: pc degradation; mt: murine tissue; ca: cartilage; sp: sponge). (e, f) Human origin of invading cells was confirmed by species-specific antibodies against vimentin (e) or proMMP-13 (f) (red arrows). The invasion zone was not stained by murine-specific IL-1R antibodies (g), in contrast to murine vessels (black arrows). Phase contrast shows the non-stained invasion zone (green arrows).

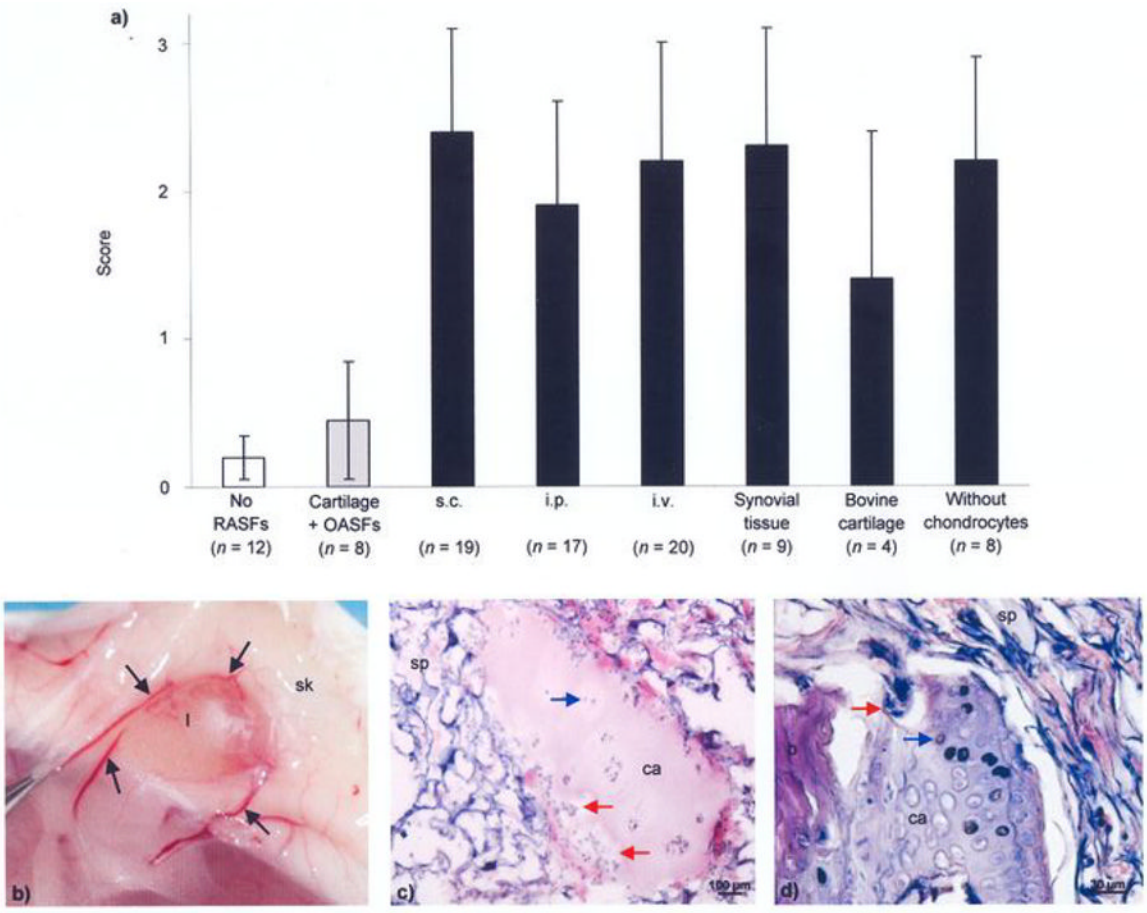

Figure 2. Migratory potential of RASFs

(a) Invasion scores of cartilage after s.c., i.v., i.p. injection, implantation of whole synovium, bovine cartilage and cartilage without viable chondrocytes, showing a strong invasion in contrast to OASFs and implants without RASFs.

(b) Neovascularization 7 days after implantation. I: Implant; sk: murine skin; black arrows: murine vessels.

(c) Migration of human RASF out of synovial tissue into RASF-free cartilage (red arrows: invasion; blue arrow: pc degradation).

(d) Invasion of implanted murine articular heads was mainly observed at the cartilage-bone junction (red arrow; blue arrow: pc cartilage degradation; ca: cartilage; b: bone; sp: sponge).

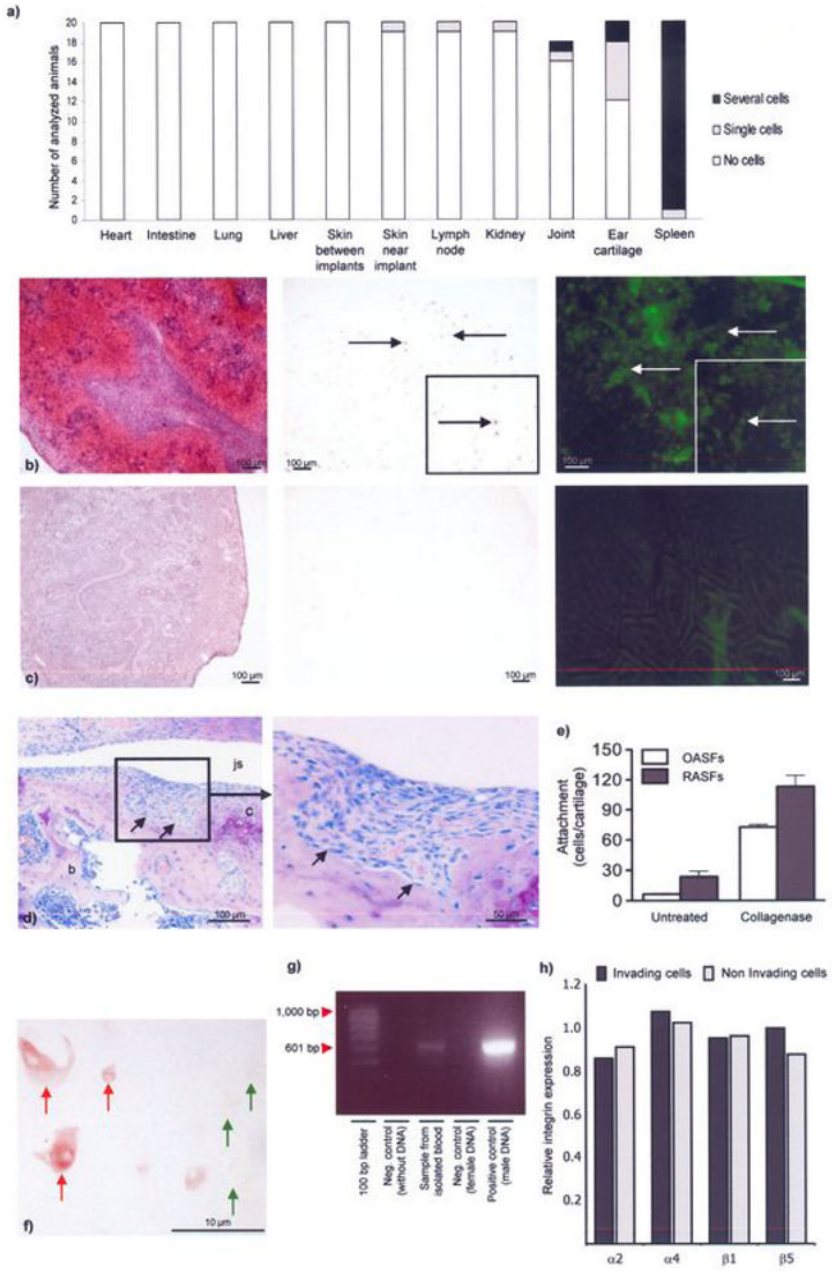

Figure 3. Migration and adhesion of RASF *in vitro*

(a) Several RASFs (black bars) were detectable in murine organs, particularly in the spleen and ear cartilage (grey bars: single RASFs; white bars: no RASFs). (b) Immunohistochemistry for human vimentin showed RASFs in the spleen (b) but not in the intestine (c). Left: hematoxylin-eosin staining; center: vimentin-stained RASFs (black arrows); right: EGFP-transduced RASFs (white arrows).

(d) After collagenase treatment and injection of RASFs, invasive erosions (arrows) were detectable in the damaged articular cartilage surface (day 39 after injection; c: cartilage; b: bone; js: joint space).

(e) Increased adhesion of RASFs seeded on collagenase-treated and non-treated human cartilage in comparison to OASFs and towards collagenase-digested cartilage when compared to intact cartilage.

(f) Vimentin-positive RASFs are present in the murine blood, showing a remarkably high amount of human cells in this sample (n = 2); red arrows: RASFs; green arrows: murine cells.
(g) y-chromosome-specific RASF-derived *sry*-fragment was detectable in isolated DNA out of murine blood and in the positive control. Estimated size of the *sry*-fragment: 601 bp.
(h) No difference in expression of integrin-subunits between invading/non-invading or primary/contralaterally implanted RASF was observed by real time-PCR after LMM.

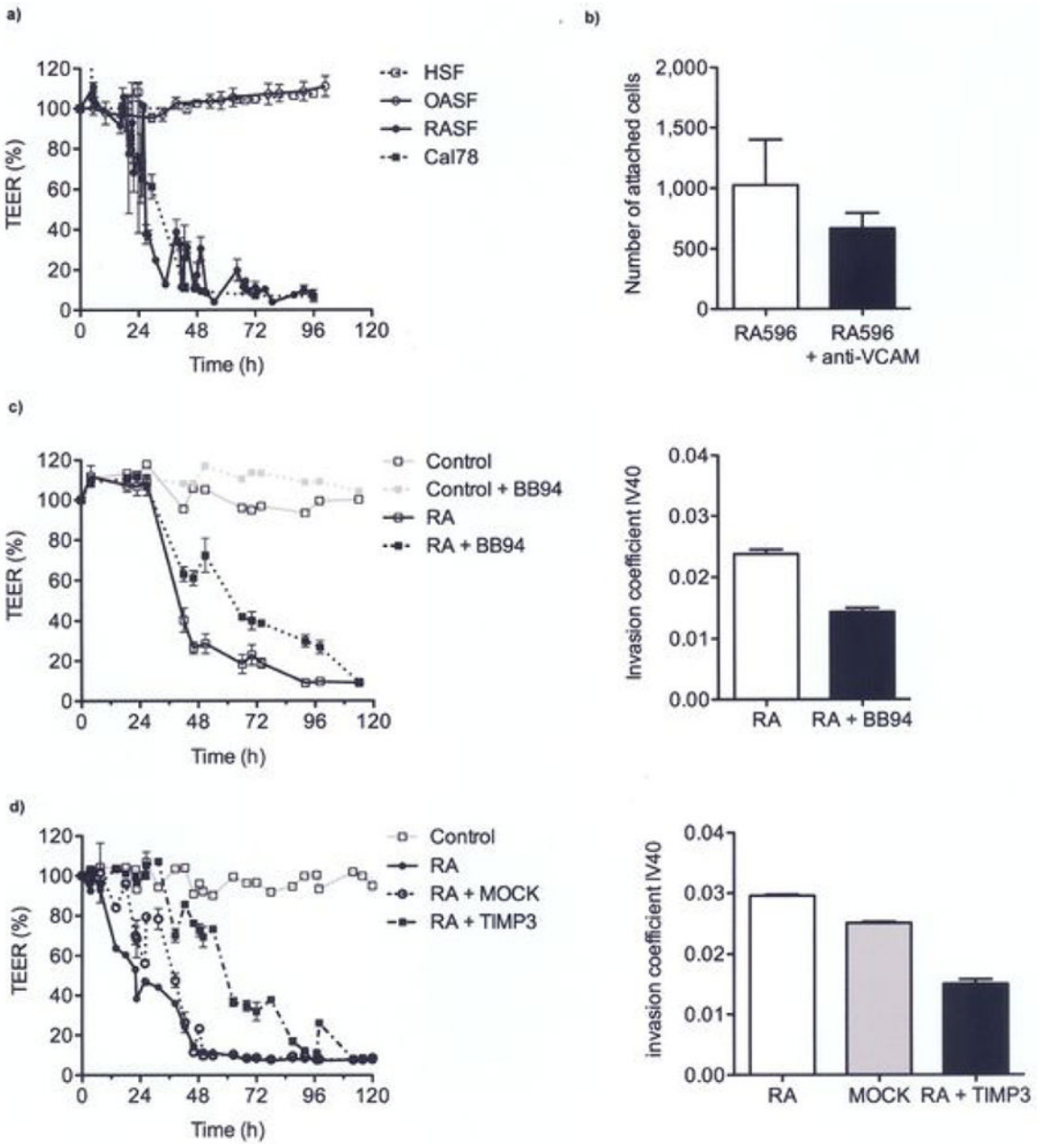

Figure 4. RASF-transmigration and inhibition *in vitro*

(a) RASFs showed an increased transmigratory and invasive potential in the TEER assay (n = 5 different primary cultures) through MDCK-C7 monolayers, comparable to Cal78 cells. HSF and OASF (n = 3 different primary cultures) showed no transmigratory behavior. p<0.05 for RASFs and Cal78 vs. HSFs and OASFs, respectively.

(b) Cell adhesion was inhibited by RASF-treatment with anti-VCAM-1 antibodies. The transmigratory potential of RASFs (TEER assay) was decreased by treatment or transduction of RASFs with BB-94 (c) and TIMP-3 (d). P<0.05 for RASF transduced with BB94 and TIMP-1 vs. non-transduced RASFs.

Table 1

Scoring results of invasion and perichondrocytic (pc) degradation of SCID mice implants

	implant	invasion (mean ± s.d.)	pc degradation (mean ± s.d.)
Simultaneous implantation of the primary and contralateral implants (*n* = 25)	primary	2.3±0.8	1.8±0.8
	contralateral	1.9±0.9	1.6±0.6
Implantation of cartilage without cells		0.2±0.15	0,1±0,07
Implantation of OASFs together with human cartilage (*n* = 8)	primary	0.5±0.3	0.9±0.4
	contralateral	0.5±0.4	0.9±0.4
Implantation of human cartilage, implant on the contralateral side without a sponge (*n* = 3)	primary	1.2±0.5	1.8±0.5
	contralateral	2.1±0.2	2.2±0.7
Initial implantation of the contralateral implant (without RASFs); primary implant after approx. 14 days (*n* = 13)	primary	1.8±0.7	2.3±0.7
	contralateral	2.8±0.5	2.5±0.7
Initial implantation of the primary implant (with RASFs); contralateral implant after approx. 14 days (*n* = 10)	primary	2.7±0.4	2.5±0.7
	contralateral	1.5±0.6	1.7±0.8
Implantation of rheumatoid arthritis synovium and cartilage (*n* = 9)		2.3±0.8	2.0±0.5
Implantation of cartilage and subcutaneous RASF injection after approx. 14 days (*n* = 19)		2.4±0.7	2.1±0.7
Implantation of cartilage and intraperitoneal RASF injection after approx. 14 days (*n* = 17)		1.9±0.7	1.8±0.7
Implantation of cartilage and intravenous RASF injection after approx. 14 days (*n* = 20)		2.2±0.8	2.0±0.8
Subcutaneous injection of RASFs and implantation of cartilage after approx. 14 days (*n* = 3)		1.9±0.8	1.8±0.8
Intraperitoneal injection of RASFs and implantation of cartilage after approx. 14 days (*n* = 2)		1.1±0.5	1.3±0.3
Intravenous injection of RASFs and implantation of cartilage after approx. 14 days (*n* = 4)		1.6±1.2	2.0±0.7
Implantation of cartilage without viable chondrocytes (*n* = 8)		2.2±0.7	-
Implantation of bovine cartilage (*n* = 4)		1.4±1.0	1.8±0.4
Implantation of human cartilage and injection of TNFα-inhibitor (*n* = 13)		1.7±0.8	1.5±0.7

The mean values and standard deviations (s.d.) of all implants were calculated. Scoring was performed by five different trained researchers.

- : not evaluable, no viable chondrocytes; *n*: number of evaluated implants

Table 2

Summary of detected RASFs in the organs of SCID mice

Organ	no cells	single cells	few cells
Heart	20	-	-
Spleen	-	1	19
Lung	20	-	-
Liver	20	-	-
Intestine	20	-	-
Kidney	19	1	-
Lymph node	19	1	-
Skin (near the implant)	19	1	-
Skin (between implants)	20	-	-
Ear cartilage	12	6	2
Joint	16	1	1

All organs and blood samples were collected from 20 animals and used for the detection of RASFs (human cells) in the respective tissues. Of note, human cells could be detected in all spleens analyzed. Single or few cells could be detected next to the ear cartilage and the joints.

- : not detectable